



INTERNATIONAL ATOMIC ENERGY AGENCY
UNITED NATIONS EDUCATIONAL, SCIENTIFIC AND CULTURAL ORGANIZATION



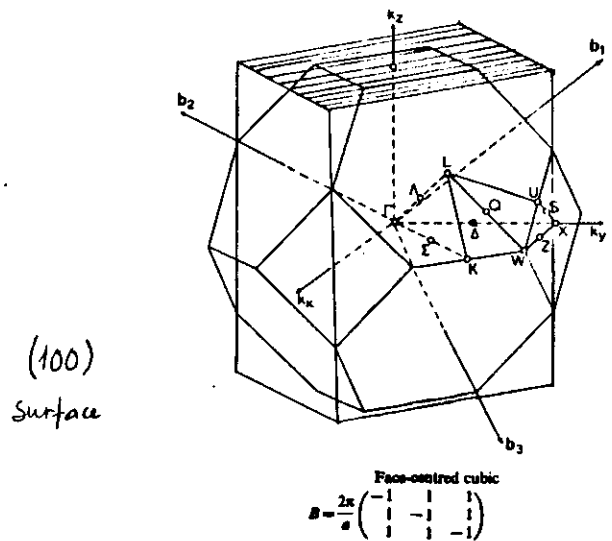
INTERNATIONAL CENTRE FOR THEORETICAL PHYSICS
34100 TRIESTE (ITALY) - P.O.B. 503 - MIRAMARE - STRADA COSTIERA 11 - TELEPHONE: 2240-1
CABLE: CENTRATOM - TELEX 460392-1

SMR/291-7

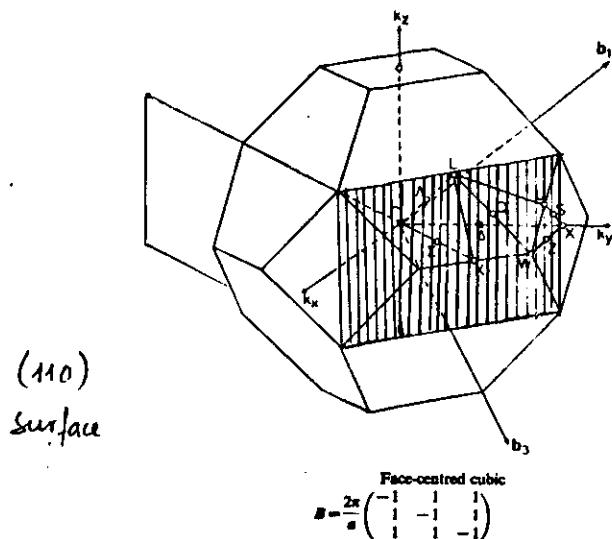
SPRING COLLEGE IN CONDENSED MATTER
ON
"THE INTERACTION OF ATOMS & MOLECULES WITH SOLID SURFACES"
(25 April - 17 June 1988)

BASIC STRUCTURAL AND ELECTRONIC PROPERTIES OF
SEMICONDUCTOR SURFACES
(Continued)

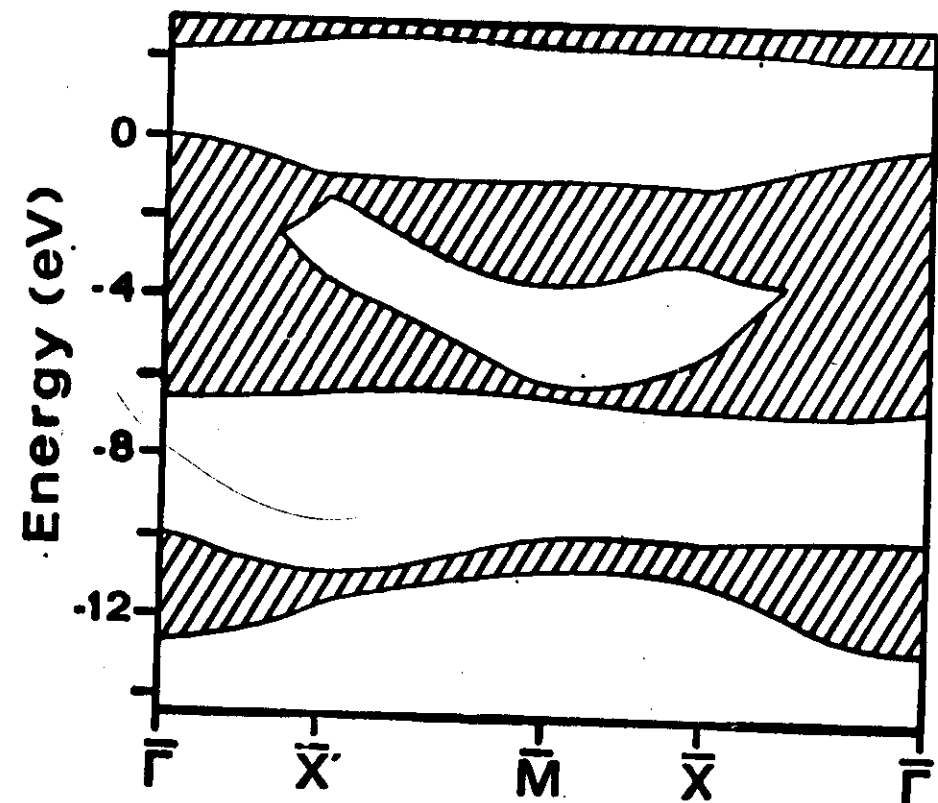
C.M. BERTONI
Dipartimento di Fisica
II Università di Roma
Via Orazio Raimondo
00173 Roma
Italy



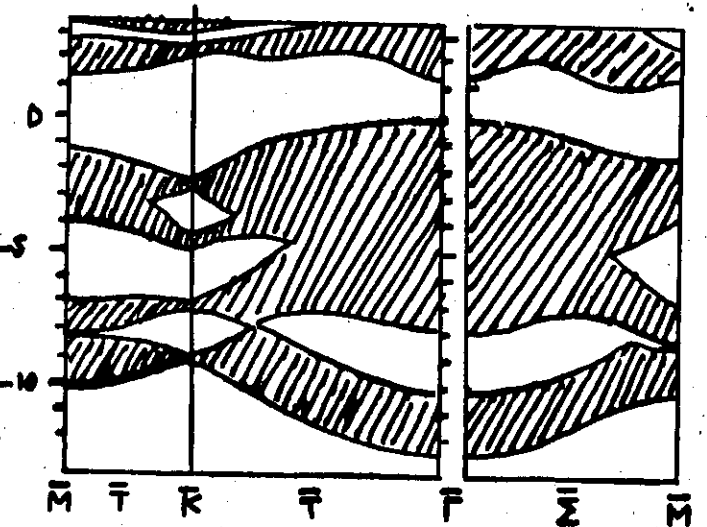
Refolding of the 3DBZ for the FCC structure into a prismatic shape leaving the 2DBZ as its basis (shaded area). The high of the new B2 $4\pi/a$, since $a/2$ is the distance between two planes of the same sublattice.



2DBZ for H0 surface. One should refold the 3DBZ into a solid having the shaded figure as its basis -



The projected bulk band structure along the symmetry directions of the 2DBZ of (110) surface of GaAs -



Projected bulk band structure of ideal (111) surface of Si, obtained in a Wigner-Seitz TB parametrization scheme.

3. Methods of Calculation. 3.1 - Density functional approach. 4

In this section we will present the ingredients of a modern surface band structure calculation. We will consider the use of self-consistent pseudopotential method in the framework of the density functional theory (DFT)⁸. The electronic properties of the ground state can be described in this framework and a set of single-particle equation can be derived⁹ in order to obtain the particle density $n(\vec{r})$ and the total energy. The eigenvalues of these one-particle Kohn-Sham equation⁽⁹⁾, can be considered (in analogy of the equations of Hartree-Fock method) the excitation energies of the system.

It has been recently pointed out that this approach is not adequate to describe the single-particle excitation of the system, especially in the case of semiconductor where the gap between empty and filled states turns out to be underestimated.⁽¹⁰⁻¹¹⁾ However the DFT and, in particular, the density approximation (LDA) of exchange-correlation term remains the most common tool to describe the electronic structure.

In the DFT the total energy is written as a functional of the electron density $n(r)$

$$E[n] = \int V(\vec{r}) n(\vec{r}) d\vec{r} + \frac{e^2}{2} \int d\vec{r} d\vec{r}' \frac{n(\vec{r}) n(\vec{r}')}{|\vec{r} - \vec{r}'|} + T_0[n] + E_{xc}[n] \quad (3.1)$$

where $V(r)$ is the external (ionic or atomic) potential, $T_0[n]$ is the kinetic energy of a system of non-interacting electrons with a particle density $n(\vec{r})$, and E_{xc} is the exchange-correlation energy. This term is assumed to be universal functional of the density. $E[n]$ achieves its minimum value for the ground state - To minimize $E[n]$ one can choose a form

$$n(\vec{r}) = \sum_k |q_k(\vec{r})|^2 \quad (3.2)$$

The problem of minimization is then transformed into the solution of a system of N one-particle equations

$$\left\{ -\frac{\hbar^2}{2m} \nabla^2 + V(r) + e^2 \int d\vec{r}' \frac{n(\vec{r}')}{|\vec{r} - \vec{r}'|} + V_{xc}(\vec{r}) \right\} q_k(\vec{r}) = \epsilon_k q_k(\vec{r}) \quad (3.3)$$

where $V_{xc} = \frac{\delta E}{\delta n}$ is the functional derivative of the exchange correlation energy. The eigenvalues and eigenfunctions of (3.3)

5

must be determined self-consistently through (3.2) and they are obtained through an iterative procedure, which ends with a total effective potential "consistent with the particle density, which comes out from solution of the equation. At each step of the procedure a new output potential is determined and compared with the input potential. The total energy becomes:

$$E = \sum_k E_k - \frac{e^2}{2} \int d\vec{r} d\vec{r}' \frac{n(\vec{r})n(\vec{r}')}{|\vec{r}-\vec{r}'|} + E_{xc}[n(\vec{r})] - \int V_{xc}(\vec{r}) n(\vec{r}) d\vec{r} \quad (3.4)$$

where the sum is limited to the first N (occupied) states, taking into account spin degeneracy. The exchange and correlation potential is commonly assumed to be a local function of the particle density. This approximation is correct only if the density is slowly varying from its average value. The form of the local functional dependence of E_{xc} is chosen from the computed exchange-correlation energy density for an uniform electron system

$$E_{xc}^{LDA}[n] = \int n(\vec{r}) E_{xc}[n] d\vec{r} \quad (3.5)$$

$$V_{xc}^{LDA}(\vec{r}) = E_{xc}[n(\vec{r})] + n(\vec{r}) \frac{dE_{xc}}{dn} \quad (3.6)$$

One of the forms commonly used in the literature for E_{xc} is given for different densities by Ceperley and Alder.¹²

A more appropriate description, beyond the LDA, would be a form

$$E_{xc} = \int d\vec{r} \int d\vec{r}' \frac{n(\vec{r})n(\vec{r}')G(\vec{r}, \vec{r}')}{|\vec{r}-\vec{r}'|} \quad (3.7)$$

where $G(\vec{r}, \vec{r}')$ is the two-particle correlation factor ; $n(\vec{r}')G(\vec{r}, \vec{r}')$ being the exchange and correlation hole; this would introduce in non-uniform systems an intrinsic non-local dependence of $V_{xc}(\vec{r})$ on $n(\vec{r})$.

¹²⁾ The total effective potential is the sum of the last three terms in the brackets of eq. 3.3 and can be considered as the potential seen by an electron.

6

Gunnarsson and Jones proposed a model form for (3.7), and consequently for V_{xc} , which has the advantage of reproducing the correct asymptotic behaviour of the exchange-correlation potential in a system of electrons confined by a surface.¹³ Out of the surface the effective potential must approach the vacuum level with the image potential form of the type $1/\vec{r}$. For the case of a semiconductor having static dielectric constant ϵ the behaviour is

$$V_{xc}(z) \approx -\frac{\epsilon-1}{\epsilon+1} \frac{e^2}{4\pi} \quad (3.8)$$

This behaviour can give origin to a new type of surface states: the image states, mainly localized in the region immediately out of the surface plane, if the wavefunction can match an internal decaying state—the energy eigenvalues can be located within 1eV from the vacuum level, so they are empty states and can be observed experimentally by inverse photoemission and by tunneling spectroscopy. The Non-Local approximation for V_{xc} is not easy to handle especially in the case of surfaces, so that only recently it has been used in a surface calculation.¹⁴

In the previous line we have implicitly adopted the point of view (not completely justified) of considering E_i like excitation energies (i.e. directly comparable to spectroscopic results) of particle (empty states) and hole (occupied states). This could be done if, instead of equations (3.3) one would have written¹⁵

$$\left\{ -\frac{\hbar^2}{2m} \nabla^2 + V(r) + e^2 \int d\vec{r}' n(\vec{r}') \frac{1}{|\vec{r}-\vec{r}'|} \right\} \psi_k(\vec{r}) + \int d\vec{r}' \Sigma(\vec{r}, \vec{r}', E) \psi_k(\vec{r}') = E_k \psi_k(\vec{r}) \quad (3.9)$$

where the self Energy Σ , non local and energy dependent, replaces the operator $V_{xc}(\vec{r}') \delta(\vec{r}-\vec{r}')$. The energy eigenvalues are the true quasiparticle energies and they can have an imaginary part, i.e. a finite lifetime. In the last year band structure calculation

using an approximate form of Σ have been performed, mainly in bulk cases, for semiconductors. The problem of the gap underestimation (which comes out clearly in a LDA calculation with good form¹⁶ for ex and wide basis set of functions and is only slightly reduced by the inclusion of nonlocality¹⁵) is overcome by the use of eq. (3.9), the difference of the two pictures being an increase, respect to DFT value of the gap by an amount ΔE , which may be very crudely approximated by a constant scissor operator A .^{**}

7

3.2 - Pseudopotential calculations and use of the repeated slab method.

To enter the problem of surface structure calculations we must note that the presence of atoms and the termination of the crystal is contained in the external potential $V(\vec{r})$ which should describe a terminated stack of atomic planes. If one wants to avoid the problem of all-electron calculation, it is possible to use the pseudopotential method for valence electrons. $V(r)$ is the superposition of ionic pseudopotential. In order to use plane wave basis set and to eliminate the complicated problem of three dimensional matching at the surface, it is convenient to use the repeated slab method. A number of atomic planes stacked with a sufficiently thick slab of vacuum is repeated periodically in order to preserve the

^{**}) The DFT calculation is completely satisfying for the calculation of the total energy of the ground state and other ground state properties. An improvement of the values of the gap can be obtained by the use of the Slater form for V_{xc} $V_{xc} = -\frac{\alpha^2 e^2}{2\pi} (3\pi^2 n(r))^{1/3}$ with $\alpha \approx 1$. This choice produces worse values of total energy.

features of a \vec{q} -space 3D calculation. The unit cell contains the whole slab of atomic planes (typically from 10 to 15) plus an empty region with a width corresponding to $4 \div 8$ missing atomic planes. If L is the thickness of the repeated slab the values of G_2 are in $\frac{2\pi}{L}$. The 3D lattice is then extremely dense of \vec{q} vectors along z . The repeated slab method has been widely used in the last years in pseudopotential calculation for semiconductor surfaces. If the thickness of the repeated slab is sufficiently high the main features of surface and bulk are well accounted for. The output of the calculation are bands for the repeated slab evaluated at $\vec{k} = (k_{||}, k_z=0)$ - Groups of bands correspond to bulk continua of states, which become a discrete sequence for the effect of the repeated slab. Surface states and resonances can be identified looking to the wavefunctions (with strong localization at the surface) and the energy locations respect to the gaps of the projected bulk band structure. We must note that around first principle LDA calculations other method have been used adopting repeated slab method. See applications of LAPW and of LMTO. These methods in the case of semiconductors requires an introduction of a number of empty spheres inserted in the most open regions of semiconductor structure, in order to obtain realistic results¹⁶.

In the pseudopotential scheme the major difficulty comes from the high number of plane waves. Part of these can be treated in a perturbative way, by using Löwdin techniques. Recently this problem has been partially skipped by improving matrix-diagram iteration methods. The evaluation (3.2) of the particle density at each step of the self-consistent potential is done with a set of a few special k_y -points.

8

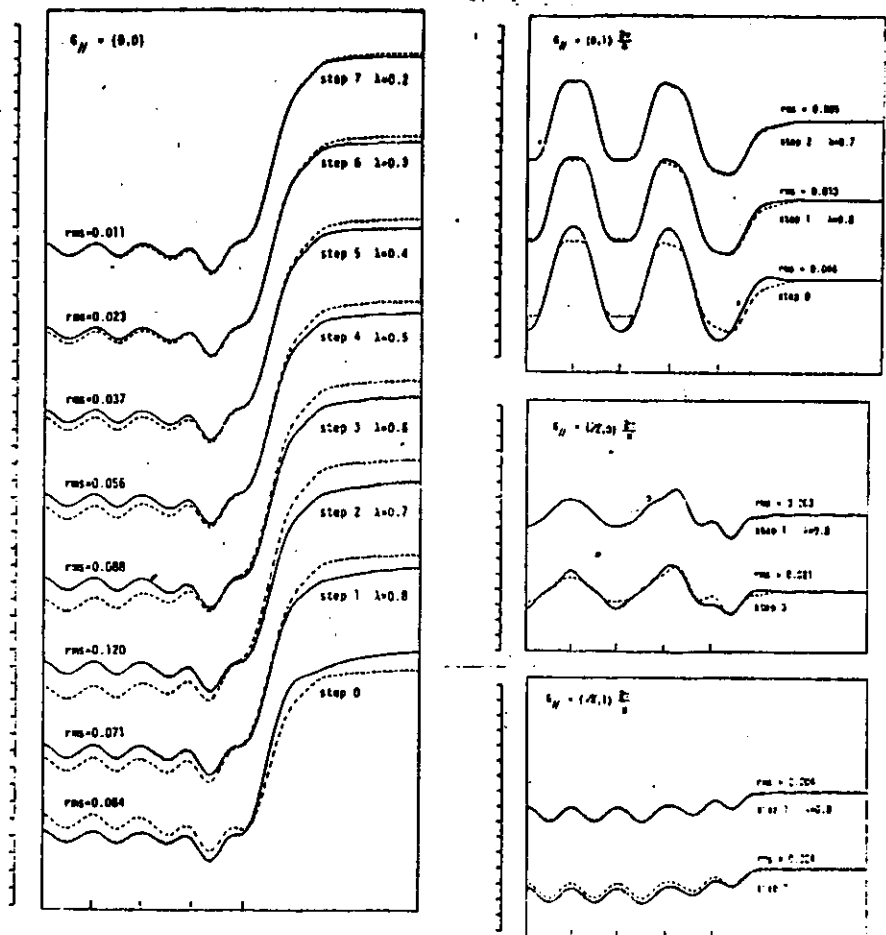


Fig. 4

In fig. following it is shown the profile $V(z)$ of the laterally averaged effective potential at different steps of the iterative procedure. Instabilities are avoided through a mixing of input and output potential via a memory factor λ - Very rapid is the convergence of $V_{\text{eff}}^{\text{av}}(z)$ with $G_{11}^{\text{av}} \neq 0$.¹⁷

The base potential $V(r)$ is a superposition of atomic pseudopotentials located at each atomic sites - the starting potential is built by a superposition of screened pseudopotential + the $V_{xc}(z)$ profile obtained for the jellium surface at the same electronic density.

3.3 - The relaxation of the cleavage surface of III-V compounds.

Before treating the detail of a specific calculation we recall some aspects of the III-V cleavage surfaces, in particular GaAs. Many experimental results and the outcome of theoretical calculations for ideal (110) surfaces, seemed to give evidence in the early seventy of the existence of two band of surface states inside the gap - Electrical measurements (contact potential differences) indicated the pinning of the Fermi level at the surface in many sample; intrinsic surface states could have been responsible - the excitation of 3d Ga electron toward the empty states, through photons or electron energy loss, gave evidence of a final state whose energy should have been in the gap. These two facts were consistent with the outcome of calculation performed for the ideal surface in the semi empirical TB scheme and using a finite slab, but this picture was misleading.

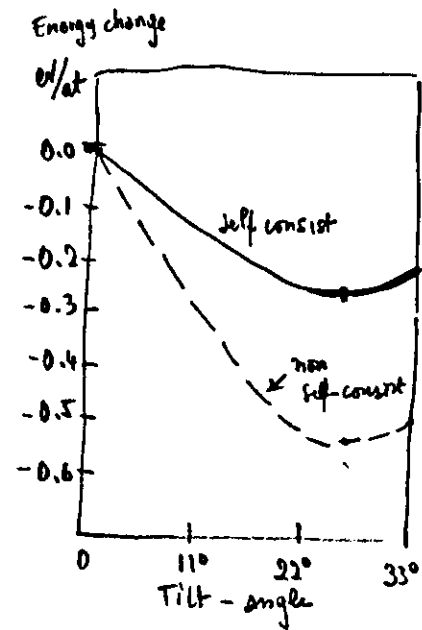
It was possible to see that the states filling the Fermi level were not intrinsic states but defects states due to bad cleavages or due to extrinsic states (contamination and absorption). Later on it was solved the problem of the $3d \leftrightarrow$ surface state excitation. The low energy of this excitation was due in part to the surface large exciton energy, probably some tenth of E_V , and in part to an upward shift of $3d$ levels at the surface layer. The gap of GaAs and of many others III-V where free of surface states if the extrinsic states due to cleavage defects were not present.

In the same years an accurate comparison between experimental and calculated LEED intensity profiles, gave indication of the relaxation of GaAs(110) surface. A rotation model¹⁸ of relaxation which produced the displacement outward of As and inward of Ga at the first plane was proposed (see Fig.). Later it was clear that a similar relaxation was common to the whole families of III-V and II-VI . An accurate review is given in Ref 19.

In the meanwhile calculations performed with different methods^{20,21} shown that this relaxation induced a shift of the two surface band. The As derived low bands was moved down in energy and the other Ga-derived empty was moved up. This was essentially due to dehybridization effects. Going down toward the second plane the atom was bonded through three bonds of $s p_3$ type, the dangling bond becoming more p_x-p_z . The As atom, going upward, changed its hybridized bond orbitals with a p -type configuration of the three bonding orbitals.

This shift of surface bands out of the gap was not only a consequence of a relaxation but the reason of the relaxation itself in term of total energy; the shift of

the occupied band toward lower energy reduces the term $\sum_K E_K$ in (3.4) respect to the ideal surface, and this shift is only in part balanced from the increase of electrostatic energy due to the growth of the distance of two atoms carrying fractional charges of different signs. The results for total energies are indicated in the figure for GaAs.²²



This relaxation is present for all III-V 's compounds and works to remove the states from the gap. In the only case of GaP, it seems possible that the relaxation is unable to remove the band of empty state out of the gap. This result obtained already in a TB calculation (see Fig.) in 1978, has been confirmed in a pseudopotential calculation and seems consistent with experimental data.

3.4 - Pseudopotential description of surface electronic structure of GaP(110).

The following Figs. are taken from Ref 23

bulk band structure
obtained with a potential
by Troullier Krömer
and Slater form for V_{XC}

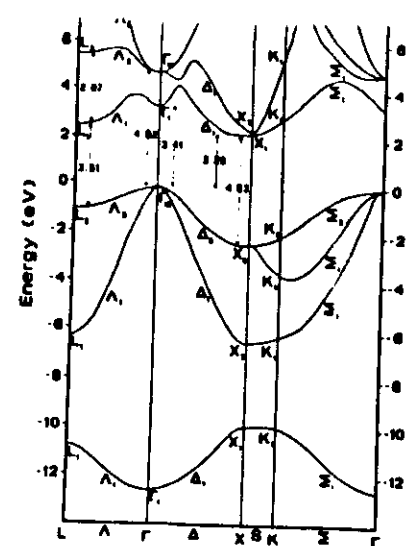


FIG. 3. Self-consistent bulk band structure of GaP.

IDEAL SURFACE
→
hole surface
and bulk states
(Comments on)
(splitting)

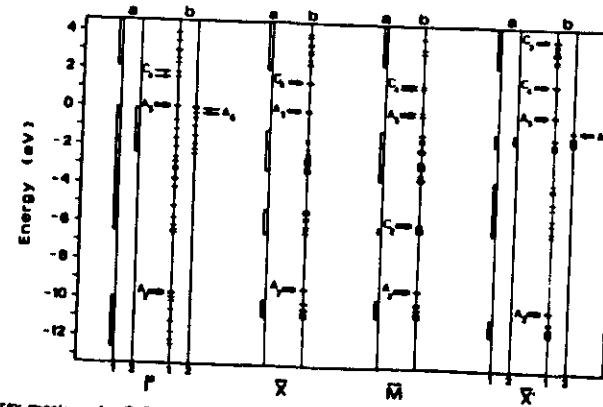


FIG. 6. Energy spectrum for GaP(110) ideal surface. Electron states are divided according to the representations of the point groups of the bulk directions corresponding to the high-symmetry points of the two-dimensional Brillouin slab calculation. Surface states are indicated by arrows and labeled by A_1 , C_1 , according to the notation of Sec. V. Energies are referred to the top of the valence band.

RELAXED SURFACE

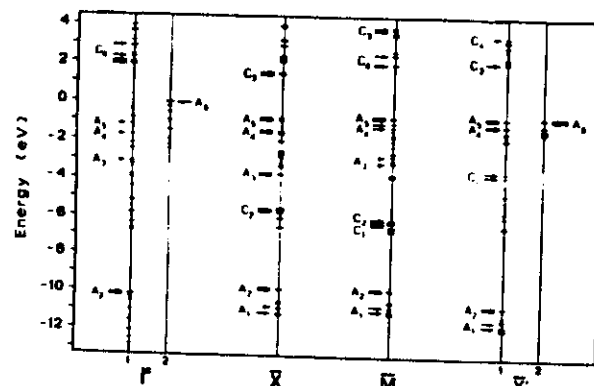


FIG. 10. Energy spectrum for GaP(110) relaxed surface.

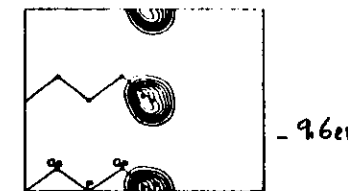


FIG. 7. Charge-density plot for surface state A_1 at M in the ideal geometry; the contours are spaced by 0.3 electrons per bulk unit cell.

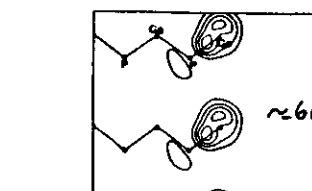
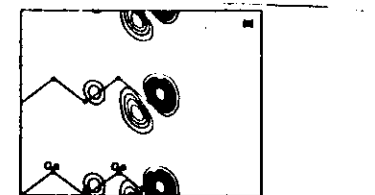


FIG. 8. Charge-density distribution of the surface state C_2 for ideal surface geometry at M .

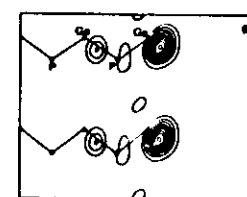


FIG. 9. Charge-density distribution for (a) filled surface state A_1 and (b) empty surface state C_1 at M point for the ideal geometry.

dangling bonds

(brick-brick empty states)

$$E \sim +3.5 \text{ eV}$$

FIG. 10. Charge-density distribution for surface state C_2 at X' in the case of ideal surface geometry plotted along a (110) plane passing through P (a) and Ga (b) surface atoms.

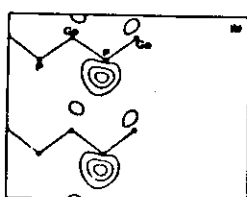




FIG. 11. Total valence charge density for relaxed GaP(110). The contours are spaced by 3.0 electrons per bulk unit cell.

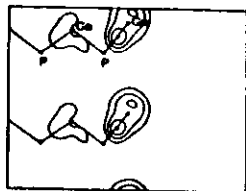


FIG. 12. Charge-density plot for state A_1 at \bar{M} point in the relaxed surface case.

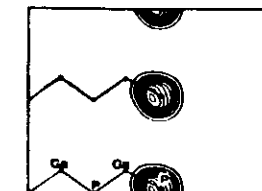


FIG. 13. Charge-density plot for A_1 at \bar{X} point for the relaxed geometry.

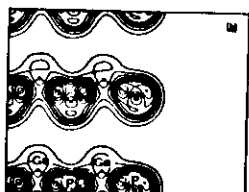


FIG. 14. Charge-density plot for state A_1 at \bar{K} point in the case of relaxed geometry.

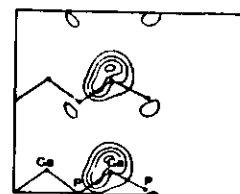


FIG. 15. Charge-density plot for state C_1 at \bar{M} point in the relaxed surface case.

FIG. 16. Charge-density distribution of surface state C_1 in the relaxed surface case.

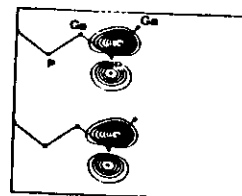


FIG. 17. Surface state A_1 , charge-density plot at \bar{X} point.

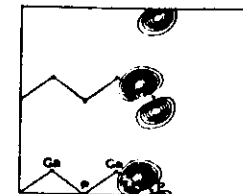


FIG. 18. Charge-density plots for (b) the dangling-bond surface state A_3 , and (c) back-bond surface state A_4 at \bar{X} point.

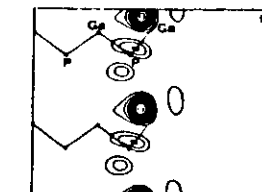
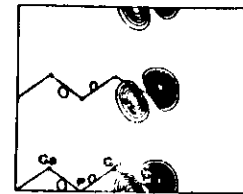
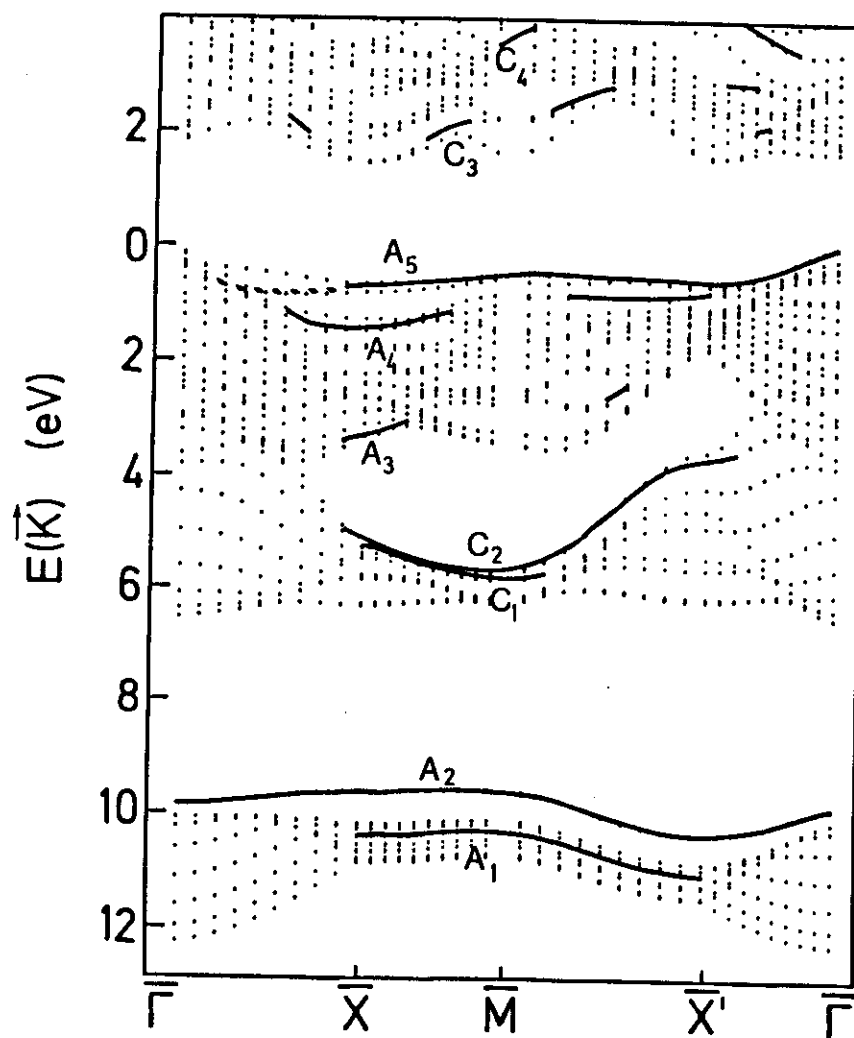


FIG. 19. Charge-density distribution for (a) C_3 and (b) C_4 surface states at \bar{M} point.

TABLE II. Energy positions referred to the valence-band maximum and parity with respect to mirror-plane symmetry of surface states found in the case of relaxed surface geometry at the high-symmetry points of the two-dimensional Brillouin zone.

	$\bar{\Gamma}$	eV	Parity	\bar{X}	eV	Parity	\bar{M}	eV	Parity	\bar{X}'	eV	Parity
A_1					-10.95	odd	-10.87	odd	-11.75	even		
A_1	-10.17	even		-8.87	even	-9.85	even	-10.74	even			
A_1	-9.13	even		-9.28	odd	-8.93	odd					
A_1	-1.72	even		-1.62	even	-1.12	even	-1.34	even			
A_1	-1.30	even		-0.88	even	-0.74	even	-0.80	even			
A_1	-0.06	odd						-0.77	odd			
C_1						-6.20	even					
C_1				-5.89	odd	-6.00	odd	-9.76	even			
C_3	1.96	even		1.83	odd	1.87	odd	2.10	even			
C_4	2.63	even				2.21	odd	3.35	even			



Band structure for GaAs(110) (unfixed),
from F. Manghi and L. Tagliorini (unpublished)

Figura 4.5 Struttura a bande per la superficie pulita di GaAs (110).

Notes on III-V cleavage surfaces:

- 1) Dispersion of even and odd surface bands have been observed along the $\bar{X}'-\bar{\Gamma}$ directions.⁽²⁴⁾ Using polarized light in photoemission experiments.
- 2) The relaxation has been confirmed by ion backscattering in blocking and channeling conditions.²⁵
- 3) The anion atom of the last plane, displaced outward is an active chemisorption site -
- 4) The two surface state (or resonance) observed in scanning tunneling spectroscopy with spatial separation -

8. P. Hohenberg and W. Kohn, Phys Rev 136 B, 864 (1964) 10)
9. W. Kohn and L.J. Sham, Phys. Rev 140 A, 1133 (1965)
10. M.S. Hybertson and S.G. Louie, Phys Rev B 34, 5390 (1986)
11. R.W. Godby, M. Schlüter and L.J. Sham, Phys. Rev Letters 56, 2415 (1986)
12. D.M. Ceperley and B.J. Alder, Phys Rev Lett. 45, 566 (1980)
13. O. Gunnarsson and R.O. Jones, Physica Scripta 21, 394 (1980)
14. F. Manghi, Phys Rev B 33, 2554 (1986)
15. F. Manghi, G. Riegler, C.M. Bertoni and G.B. Bachelet, Phys. Rev. B 31, 3680 (1985)
16. O. Bisi and S. Ossicini, not published (1988)
17. F. Manghi and E. Molinari, J. Phys C 15, 3727 (1982)
18. C.B. Duke, A.R. Kubinski, BW Lee and P. Hark, J. Vac. Sci. Technol. B13, 761 (1976)
19. A. Kahn, Surf Sci. Reports 3, 193-300 (1983)
20. J.R. Chelikowsky and M.L. Cohen, Phys Rev B 13, 826 (1976)
21. C. Calandra, F. Manghi and C.M. Bertoni, J. Phys C, 10, 1911 (1977)
22. K.C. Pandey, Phys. Rev Letters 49, 223 (1982)
23. F. Manghi, C. M. Bertoni, C. Calandra and E. Molinari, Phys Rev B 24, 6029 (1981)
24. G.P. Williams, R.J. Smith and G.J. Lapeyre, J. Vac. Sci. Technol. 15, 1249 (1978)
25. L. Smith, R.H. Tromp and J.F. van der Veen, Phys. Rev B 29, 4814 (1984)

